



UNIVERSITY OF LEEDS

This is a repository copy of *Late Permian–Middle Triassic magnetostratigraphy in North China and its implications for terrestrial-marine correlations*.

White Rose Research Online URL for this paper:

<https://eprints.whiterose.ac.uk/186497/>

Version: Supplemental Material

Article:

Guo, W, Tong, J, He, Q et al. (7 more authors) (2022) Late Permian–Middle Triassic magnetostratigraphy in North China and its implications for terrestrial-marine correlations. *Earth and Planetary Science Letters*, 585. 117519. ISSN 0012-821X

<https://doi.org/10.1016/j.epsl.2022.117519>

© 2022, Elsevier. This manuscript version is made available under the CC-BY-NC-ND 4.0 license <http://creativecommons.org/licenses/by-nc-nd/4.0/>.

Reuse

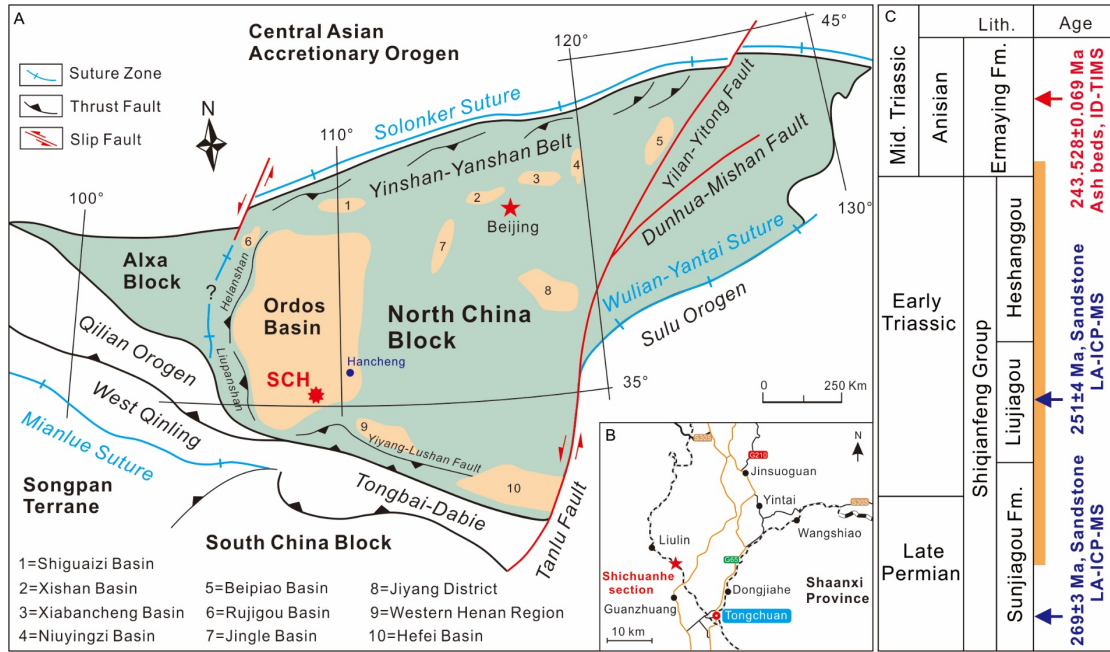
This article is distributed under the terms of the Creative Commons Attribution-NonCommercial-NoDerivs (CC BY-NC-ND) licence. This licence only allows you to download this work and share it with others as long as you credit the authors, but you can't change the article in any way or use it commercially. More information and the full terms of the licence here: <https://creativecommons.org/licenses/>

Takedown

If you consider content in White Rose Research Online to be in breach of UK law, please notify us by emailing eprints@whiterose.ac.uk including the URL of the record and the reason for the withdrawal request.



eprints@whiterose.ac.uk
<https://eprints.whiterose.ac.uk/>



1

2 Fig 1. Simplified paleotectonic map of the North China Block and its sedimentary basins (modified

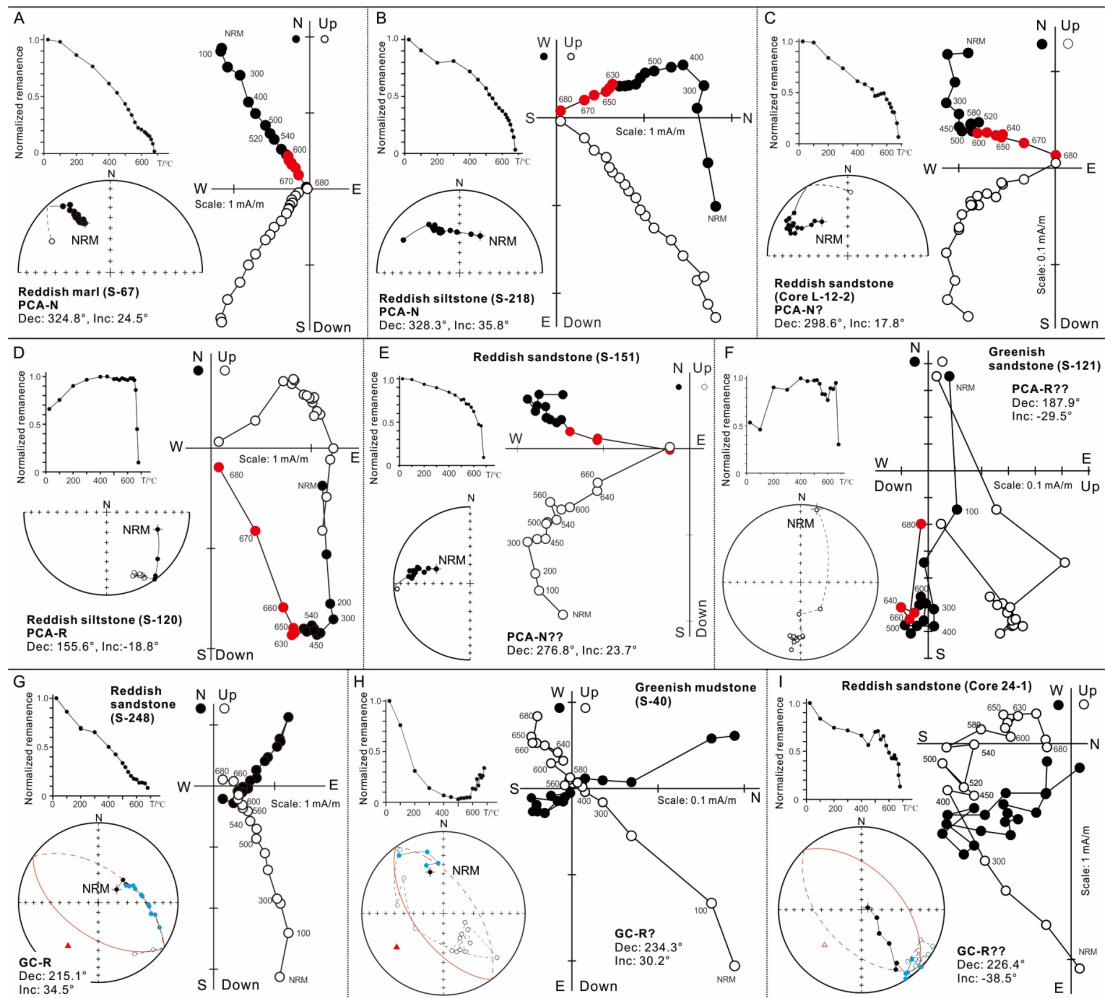
3 from Meng et al., 2019). Red star marks the studied Shichuanhe (SCH) section. Blue point indicates

4 the Hancheng section. Inset B shows a detailed location of the SCH section. C. Brief Permian–

5 Triassic chrono- and lithostratigraphic framework in North China. ID-TIMS age is from Liu et al.

6 (2018), LA-ICP-MS ages are from Zhu et al. (2019). Orange bar represents studied interval.

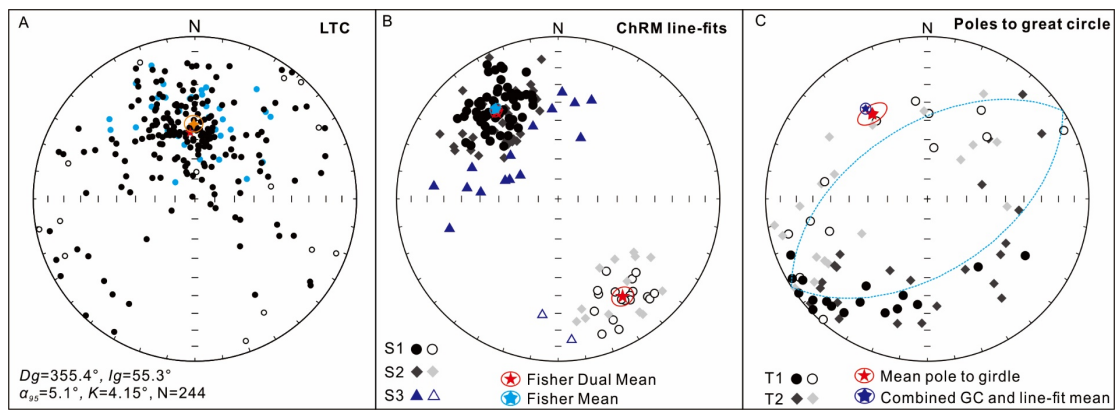
7



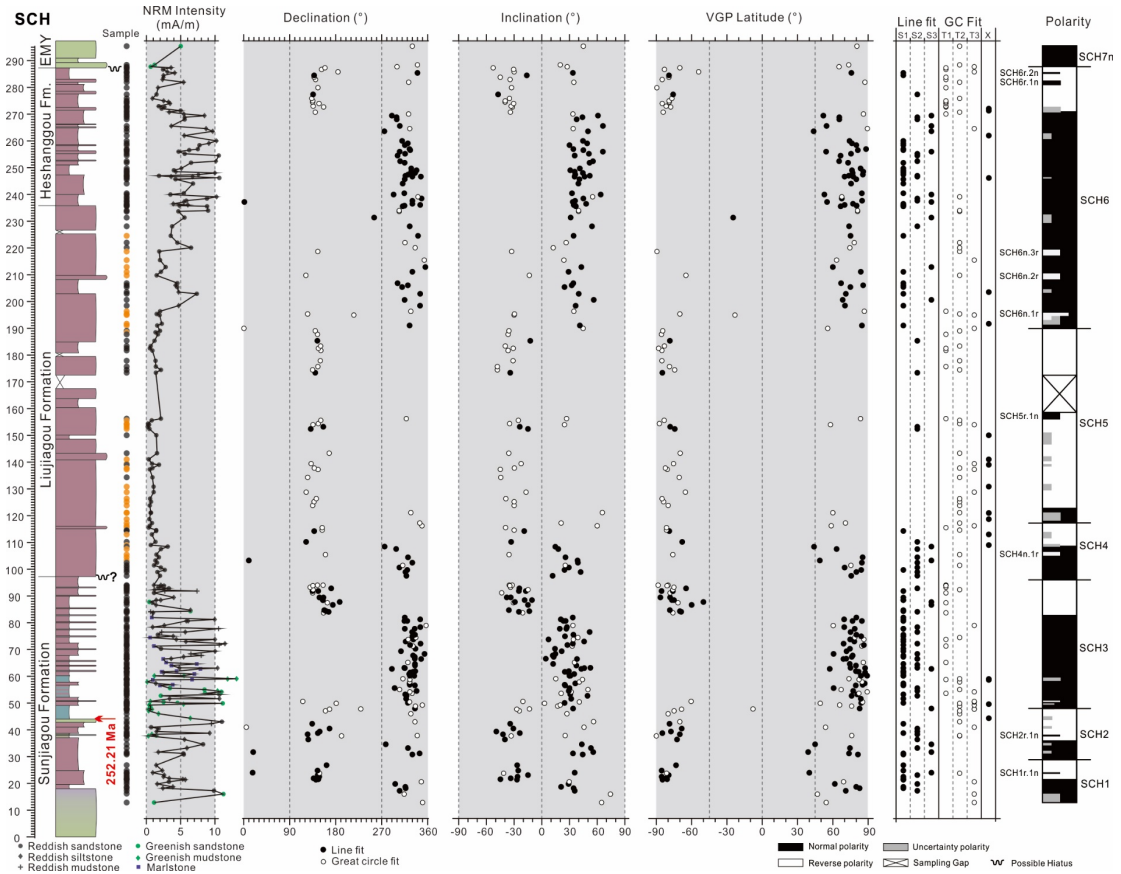
8

9 Fig 2. Representative demagnetization behaviors with polarity interpretation of specimens from
10 Shichuanhe section. A–F: Principal Component Analysis (PCA), steps used for ChRM line-fits are
11 highlighted in red. A. A largely single component magnetization shows a stable end-point that is
12 close to expected Early Triassic direction in North China (polarity N; S1 class), Sunjiagou
13 Formation. B. After removal of an eastward LTC below 400°C, specimen shows good linearity to
14 the origin with the ChRM from 630–680°C steps, polarity N (S1), Heshanggou Formation. C.
15 Similar demagnetization behavior to B, but the ChRM direction is a little deviated from expected
16 direction (N?, S2), Liujiagou Formation. D. Two component magnetizations with the ChRM 630°C
17 to the origin (R, S1). Apparent mid-stable component is from blocking temperature overlap between
18 the ChRM and the LTC, Sunjiagou Formation. E. Specimen shows good linearity above 600°C, but
19 isolated ChRM is deviated from expected direction (N??, S3), Liujiagou Formation. F. The last three
20 steps show moderately linear ChRM component and the LTC is a composite LTC and Triassic
21 reverse component (R??, S3), Sunjiagou Formation. Filled (open) symbols are lower (upper)
22 hemisphere. G–I: Great-circle (GC) fits, red arc represents fitted great circle and blue indicates

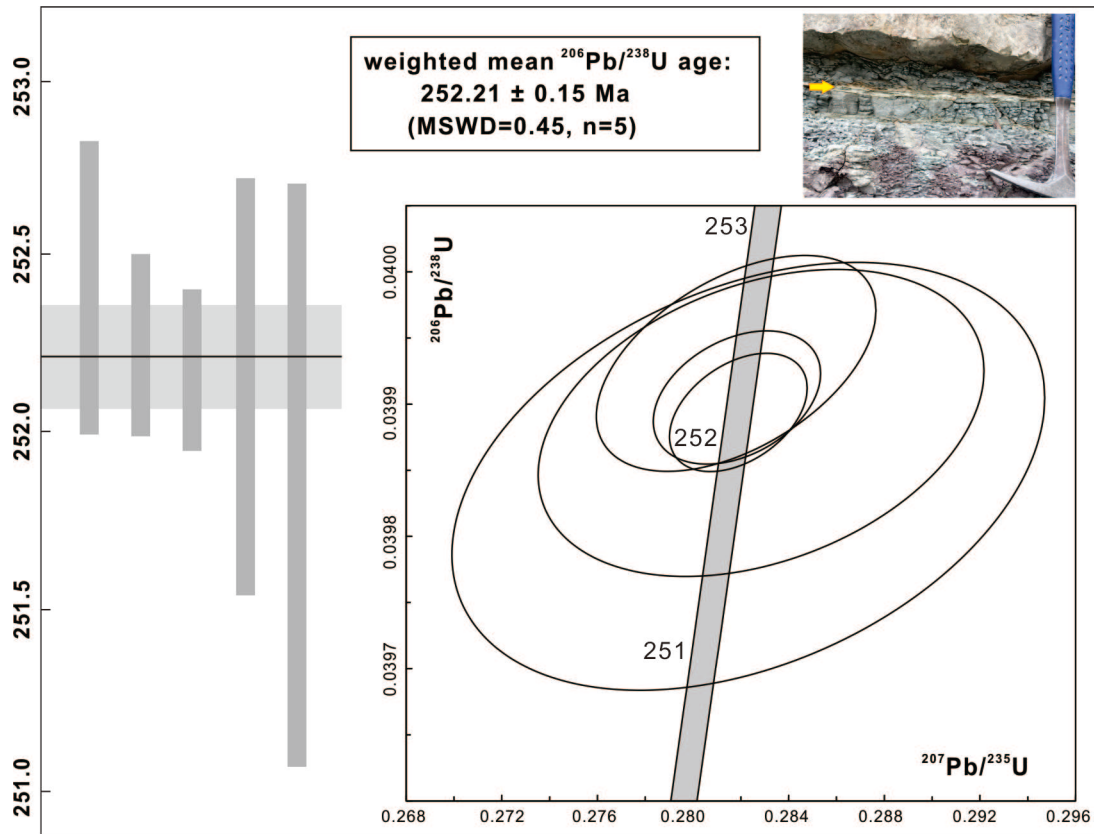
23 points used. Lower projection paths dashed and upper projection paths are solid. G. Great circle
 24 plane from 200–680°C, specimen shows unscattered great circle trend towards the expected reverse
 25 direction (R, T1). LTC (100–500°C) is likely a composite component, Heshanggou Formation. H.
 26 Well-defined LTC 100–400 °C and a somewhat scattered trend (moderate arc length 100–540°C)
 27 towards Triassic reverse, with erratic directions above 600°C, due to thermal alteration (R?, T2),
 28 Sunjiagou Formation. I. Well-defined LTC NRM–400°C and a trend towards expected Triassic
 29 reverse direction with the great circle fitted to the higher temperature steps (R??, T3), Liujiagou
 30 Formation.
 31



32
 33 Fig 3. Equal-area stereographic projection of the low-temperature components (LTC) and
 34 characteristic (ChRM) components of the Shichuanhe section. A. LTC in geographic coordinates,
 35 with the Fisher means (red star) close to the recent geomagnetic dipole field direction (orange star)
 36 at the SCH site (IGRF, computed from
 37 <https://www.ngdc.noaa.gov/geomag/calculators/magcalc.shtml#igrfwmm>). B. Dual polarity ChRM
 38 line fits (in stratigraphic coordinates), with calculated Fisher (dual) mean (only S1 and S2 data used)
 39 and Fisher means of all converted to normal (Blue star with 95% confidence ellipse). C. Poles to
 40 the great circle planes of T1 and T2 class data, along with the mean of the combined great circle and
 41 line-fits (McFadden and McElhinny, 1988). The single girdle plane (dotted) is the plane normal to
 42 the mean direction calculated using both the great circle poles and ChRM fits. Red star indicates the
 43 mean pole to the great circle girdle of points and its elliptical 95% confidence cone. The filled (open)
 44 circles refer to the lower (upper) hemisphere, respectively.



46
 47 Fig 4. Magnetostratigraphy of the Shichuanhe (SCH) section with polarity quality ratings.
 48 Demagnetization behavior of S and T refer to ChRM line-fits (filled circles) and great circle fits
 49 (open circles), respectively, which are subdivided into S1, S2, S3 and T1, T2, T3 class (see text for
 50 details). Specimens with no Triassic magnetization are marked X. Half-width bars indicate a single
 51 sample with high quality (S1, S2 or T1, T2), showing opposite polarity interpretation with respect
 52 to adjacent samples. For the gray bar, one-quarter-width means single poorest quality or
 53 undetermined polarity (S3, T3 and X), whereas half-width indicates successive poorest or
 54 undetermined polarities.
 55



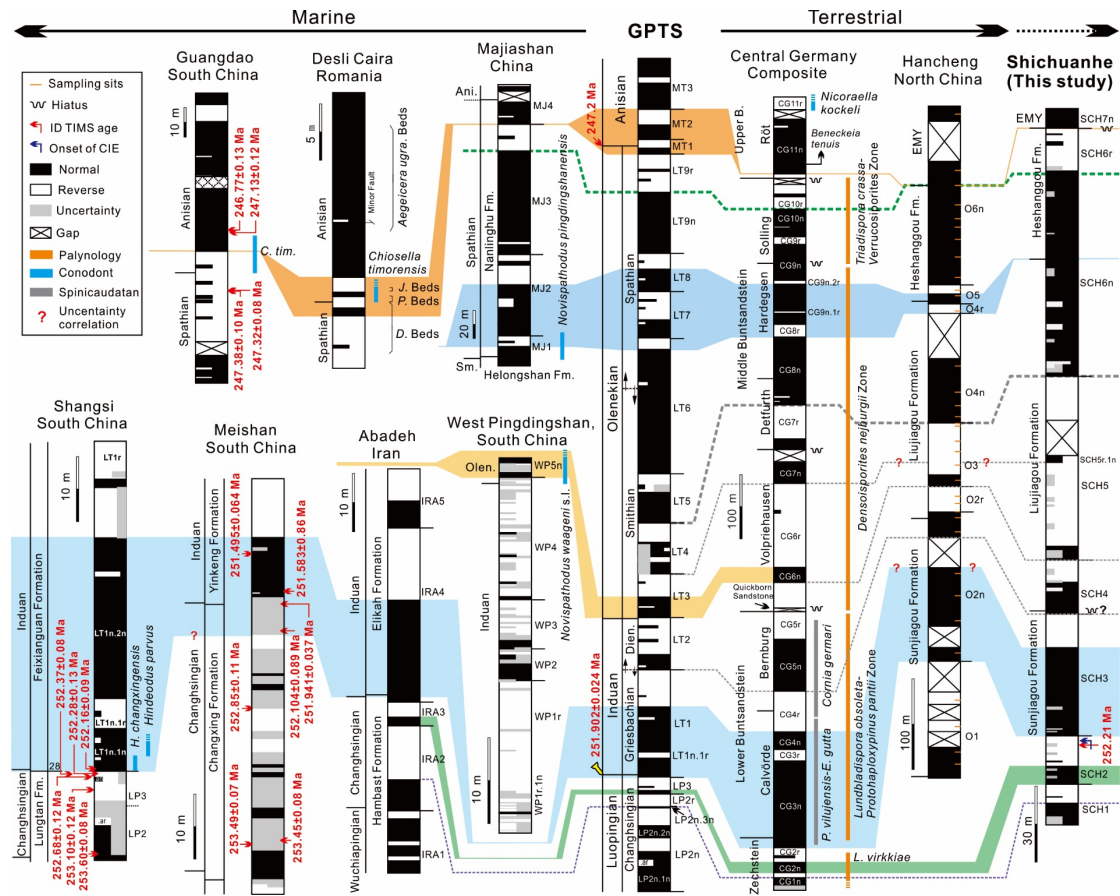
56

57 Fig 5. Concordia diagram and ranked $^{206}\text{Pb}/^{238}\text{U}$ plot of the analyzed zircon grains by the CA-ID-
 58 TIMS method from the Shichuanhe ash bed (upper right inset marked by yellow arrow). Each
 59 vertical bar represents a single zircon analysis included in the weighted mean age and the bar height
 60 is proportional to the 2σ analytical uncertainty. The horizontal black line and gray band represent
 61 the calculated weighted mean age and its 2σ analytical uncertainty envelope, respectively. Two
 62 outlier analyses excluded from age calculation plot outside the diagram area and are not shown here.
 63 See Supplementary data C for complete U-Pb data.

64

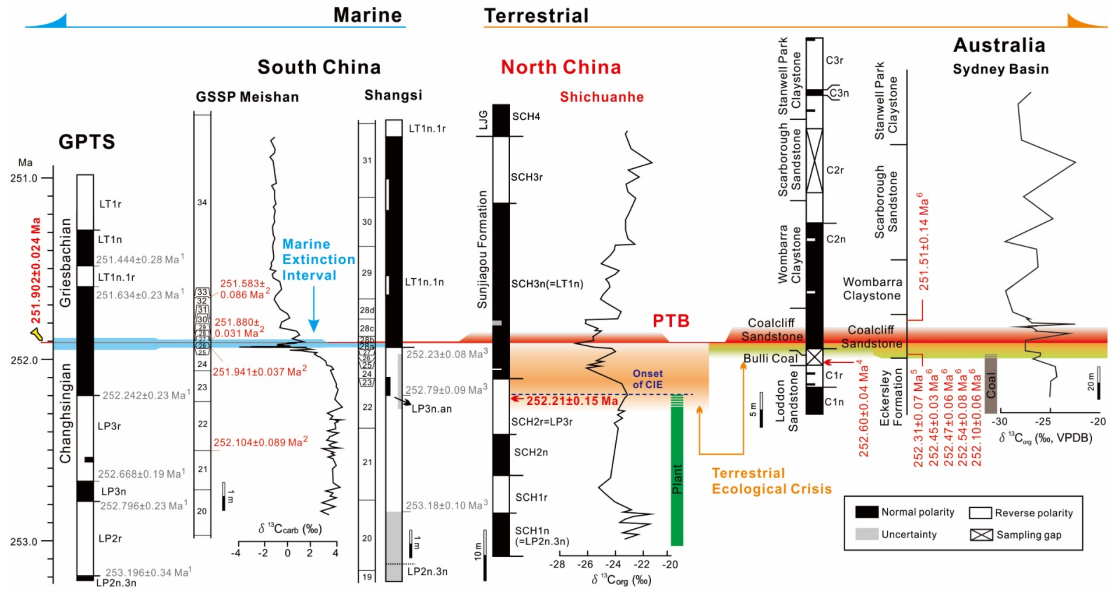
65 Table 1. Permian–Triassic mean directions and virtual geomagnetic poles for the Shichuanhe section
 66 and other sections in North China. Paleolatitude and reversal test of Yang et al. (1991) were not
 67 provided in the original study.

68



69

70 Fig 6. Changhsingian–Anisian magnetic polarity stratigraphy of North China and comparison with
 71 other non-marine and marine successions. Geomagnetic polarity timescale (GPTS) is based on
 72 Hounslow and Muttoni (2010) and Hounslow and Balabanov (2018). Compiled Central German
 73 Composite and biostratigraphy (Szurlies, 2007, 2013; Kürschner and Hengreen, 2010; Scholze et
 74 al., 2017). Hancheng section (Ma et al., 1992). Distance between sampling sites >30 m is marked
 75 by a sampling gap. West Pingdingshan (Sun et al., 2009), Majiangshan (Li et al., 2016), Meishan
 76 (Modified from Hounslow and Balabanov, 2018), Abadeh (Gallet et al., 2000; Szurlies, 2013),
 77 Guangdao (Lehrmann et al., 2006), Shangsì (Hounslow and Balabanov, 2018; Yuan et al., 2019).
 78 Desli Caira (Grădinaru et al., 2007). Question marks indicate uncertain correlations. *D.*
 79 *Beds*=*Deslicairites* Beds; *P. Beds*=*Paracrocordicera* Beds; *J. Beds*=*Japonites* Beds; *P. vilujensis*–
 80 *E. gutta*=*Palaeolimnadiopsis vilujensis*–*Euetheria gutta*; *L. virkkiae*=*Lueckisporites virkkiae* Zone.
 81



82

83 Fig 7. Correlation of the Permian–Triassic interval sequence at Shichuanhe with the GSSP at
 84 Meishan (Burgess et al., 2014), Shangsí (Yuan et al., 2019) and Australian sections (Belica, 2017;
 85 Fielding et al., 2019, 2021). Ages of ¹=calculated by Hounslow and Balabanov, 2018, ²=Burgess et
 86 al., 2014, ³=calculated magnetozone boundary ages by Yuan et al., 2019, ⁴=Metcalf et al., 2015,
 87 ⁵=Fielding et al., 2019, ⁶=Fielding et al., 2021. GPTS is from (Hounslow and Balabanov, 2018).
 88 Carbon isotope curve of Shichuanhe (Wu et al., 2020).